

## Get Clarity On Generics

Cost-Effective CT & MRI Contrast Agents



FRESENIUS  
KABI

WATCH VIDEO

# AJNR

## Dual-Layer Detector Head CT to Maintain Image Quality While Reducing the Radiation Dose in Pediatric Patients



Zhengwu Tan, Lan Zhang, Xiaojie Sun, Ming Yang, Joyman Makamure, Hongying Wu and Jing Wang

This information is current as of August 7, 2025.

*AJNR Am J Neuroradiol* published online 21 September 2023

<http://www.ajnr.org/content/early/2023/09/21/ajnr.A7999>

# Dual-Layer Detector Head CT to Maintain Image Quality While Reducing the Radiation Dose in Pediatric Patients

 Zhengwu Tan, Lan Zhang, Xiaojie Sun, Ming Yang, Joyman Makamure, Hongying Wu, and  Jing Wang



## ABSTRACT

**BACKGROUND AND PURPOSE:** Radiation exposure in the CT diagnostic imaging process is a conspicuous concern in pediatric patients. This study aimed to evaluate whether 60-keV virtual monoenergetic images of the pediatric cranium in dual-layer CT can reduce the radiation dose while maintaining image quality compared with conventional images.

**MATERIALS AND METHODS:** One hundred six unenhanced pediatric head scans acquired by dual-layer CT were retrospectively assessed. The patients were assigned to 2 groups of 53 and scanned with 250 and 180 mAs, respectively. Dose-length product values were retrieved, and noise, SNR, and contrast-to-noise ratio were calculated for each case. Two radiologists blinded to the reconstruction technique used evaluated image quality on a 5-point Likert scale. Statistical assessment was performed with ANOVA and the Wilcoxon test, adjusted for multiple comparisons.

**RESULTS:** Mean dose-length product values were 717.47 (SD, 41.52) mGy×cm and 520.74 (SD, 42) mGy×cm for the 250- and 180-mAs groups, respectively. Irrespective of the radiation dose, noise was significantly lower, SNR and contrast-to-noise ratio were significantly higher, and subjective analysis revealed significant superiority of 60-keV virtual monoenergetic images compared with conventional images (all  $P < .001$ ). SNR, contrast-to-noise ratio, and subjective evaluation in 60-keV virtual monoenergetic images were not significantly different between the 2 scan groups ( $P > .05$ ). Radiation dose parameters were significantly lower in the 180-mAs group compared with the 250-mAs group ( $P < .001$ ).

**CONCLUSIONS:** Dual-layer CT 60-keV virtual monoenergetic images allowed a radiation dose reduction of 28% without image-quality loss in pediatric cranial CT.

**ABBREVIATIONS:** CNR = contrast-to-noise ratio; CTDI<sub>vol</sub> = volume CT dose index; DECT = dual-energy CT; DLCT = dual-layer CT; DLP = dose-length product; GWMA = assessment of GM-WM differentiation; PFAA = assessment of artifacts in posterior fossa; SSA = assessment of the subcalvarial space; SAI = subcalvarial artifact index; VMI = virtual monoenergetic image

Unenhanced CT of the head is the standard technique for detecting intracranial pathologies, including trauma or intracranial hemorrhage, in children in the emergency department.<sup>1</sup> MR imaging can accurately detect traumatic complications but often requires sedation in children because of the examination


length and motion sensitivity, which limits rapid assessment; consequently, CT is considered the first-line imaging technique for suspected intracranial injury because of the short examination duration and high sensitivity for acute hemorrhage.<sup>2</sup> Because CT use in children has risen dramatically, radiation exposure from CT scanning is of an increasing concern; indeed, pediatric patients may receive high radiation doses and are more susceptible to radiation-related malignancies than adults because of organ masses, volumes, and morphology that are very different in children compared with adults.<sup>3-7</sup> Therefore, it is important to optimize the imaging parameters to be consistent with the patient's size. From the patient's perspective, the benefits of a medically required CT scan far exceed the small increase in radiation-induced cancer risk,<sup>8</sup> but it is always beneficial to reduce radiation exposure from CT scanning in children. Several strategies, eg, reducing the tube current (milliamperes) and voltage (kilovoltage) as well as using adaptive statistical iterative reconstruction to maintain image quality

Received April 7, 2023; accepted after revision August 2.

From the Department of Radiology (Z.T., L.Z., X.S., M.Y., J.M., H.W., J.W.), Union Hospital, Tongji Medical College, Huazhong University of Science and Technology, Wuhan, Hubei, China; and Hubei Province Key Laboratory of Molecular Imaging (Z.T., L.Z., X.S., M.Y., J.M., H.W., J.W.), Wuhan, Hubei, China.

This research was supported by the National Natural Science Foundation of Hubei Province, China (No. 2021CFB447).

Please address correspondence to Jing Wang, MD, Department of Radiology, Union Hospital, Tongji Medical College, Huazhong University of Science and Technology, No. 1277, Jiefang Ave, Wuhan, China; e-mail: jjwinflower@126.com

 Indicates open access to non-subscribers at [www.ajnr.org](http://www.ajnr.org)

 Indicates article with online supplemental data.

<http://dx.doi.org/10.3174/ajnr.A7999>

**Image-acquisition parameters, workstation, and viewing modes used for the evaluation**

Scanner Model	250 mAs	180 mAs
Scanner sequence	Unenhanced image	Unenhanced image
KVp/tube current	120/250	120/180
Pitch/rotation	0.390/0.5	0.390/0.5
Detector configuration	64 × 0.625	64 × 0.625
Kernel	B	B
Section thickness	1 mm	1 mm
Reconstructed thickness	5 mm	5 mm
Iterative reconstruction algorithm/level	Spectral/level 3	Spectral/level 3
Workstation	IntelliSpace 9.0 <sup>a</sup>	IntelliSpace 9.0 <sup>a</sup>
Viewing mode/VMI	MonoE	MonoE
CT dose		
DLP (mGy × cm)	717.47 (SD, 41.52)	520.74 (SD, 42.00)
DLP, 0–6 yr	711.45 (SD, 47.83)	503.76 (SD, 54.00)
DLP, 7–12 yr	724.75 (SD, 31.80)	531.88 (SD, 27.47)
CTDI <sub>vol</sub> (mGy)	36	26

**Note:**—MonoE indicates monoenergetic.

<sup>a</sup> Philips Healthcare.

while reducing radiation, are available.<sup>5,9–11</sup> However, image quality can be reduced by low signal intensity and low contrast as well as artifacts caused mainly by movement, image superimposition of different structures, and other factors.

Since the clinical introduction of dual-energy CT (DECT) with rapid kilovolt switching and dual x-ray sources that acquire 2 attenuation data sets by separating energies at the tube level, virtual monoenergetic images (VMIs) have improved soft-tissue contrast and reduced beam-hardening artifacts.<sup>12,13</sup> From a neuroimaging perspective, DECT has improved image quality and lesion characterization while reducing radiation exposure in pediatric patients.<sup>14,15</sup> A previous study of pediatric patients reported that 60-keV virtual monoenergetic imaging maximized image quality for the brain parenchyma.<sup>16</sup> A type of DECT using 2 separate orthogonally oriented x-ray spectrum source detectors generated VMIs on the basis of high- and low-energy data sets (typically at 80 kV[peak] and 140 kVp) from the same anatomic region.<sup>17</sup> However, in most patients, these dual-energy systems are operated as conventional scanners because dual-energy scanning affects scanner performance, either by neutralizing or increasing the radiation dose.<sup>18–20</sup>

Recently, a detector-based approach, referred to as spectral detector CT, was introduced with a shorter scanning time, faster postprocessing, and a lower radiation dose.<sup>18,21</sup> Dual-layer CT (DLCT) uses a single x-ray source and a detector comprising 2 scintillation layers to perform spectral separation at the detector level using the different absorption properties of the detector layers for high-energy and low-energy photons. The upper layer of the detector is yttrium-based and records lower-energy photons, while the lower layer is gadolinium oxysulfide-based and records higher-energy photons.<sup>13</sup> Another benefit of this scanning method is that the dual-energy data set is retrieved from the conventional scan and may be used for retrospective analysis. Previous data showed that the quality of GM-WM matter contrast images can be optimized,<sup>22</sup> and VMIs from spectral detector CT enabled a 19% reduction in the radiation dose in adult cranial CT while maintaining superior image quality over conventional images obtained with full-dose acquisition.<sup>23</sup> Despite

these encouraging results for adult head imaging, this technique has not been validated in the pediatric population so far.

Therefore, this study aimed to compare 60-keV VMIs with conventional images obtained with different acquisition protocols to evaluate whether a reduced radiation dose can be achieved in 60-keV VMIs without compromising image quality.

## MATERIALS AND METHODS

### Patient Population

This retrospective, single-center study was approved by the institutional ethics review board (Union Hospital, Tongji Medical College, Huazhong University of Science and Technology), who

waived the requirement for written informed consent.

A total of 148 CT brain scans were consecutively performed in pediatric patients aged 12 years or younger between December 2020 and August 2022 with a standard DLCT protocol in our clinical center. Fourteen patients were excluded from the analysis for severe encephalomalacia, which makes distinguishing GM and WM difficult ( $n = 8$ ) and artifacts that reduce image quality (eg, metal implants) ( $n = 6$ ). Then, 28 patients were excluded because of incomplete data ( $n = 28$ ). Finally, 106 patients were analyzed in this study and assigned to 2 groups according to tube current (250 and 180 mAs); they were further divided into 2 subgroups according to age (6 years or younger and >older than 6 years) (Online Supplemental Data).

### Spectral CT Examination

CT was performed with a dual-layer detector CT scanner (IQon; Philips Healthcare). In all selected patients, 53 scans were obtained with a tube current–time product of 250 mAs, and the other 53 scans, with 180 mAs. All other scan parameters were identical (Table). Conventional images were reconstructed with a hybrid algorithm (iDose4, Filter UB; Philips Healthcare iterative reconstruction algorithm). Meanwhile, 60-keV VMIs were reconstructed with a dedicated spectral image-reconstruction algorithm (Spectral, Filter UB; Philips Healthcare). Denoising was set at a minimum level (level 3 of 7) in both reconstruction approaches. All images were reconstructed using a section thickness of 1 mm and a section increment of 1 mm. The dose-length product (DLP) and volume CT dose index (CTDI<sub>vol</sub>) values were recorded on the radiation dose report.

### Objective Image Analysis

The 60-keV VMIs and conventional images were reviewed by an independent radiologist (reader 1) with 2 years of experience in head CT, and objective image analysis was performed with a proprietary vendor console (Spectral Diagnostics Suite; Philips Healthcare). The reviewers had prior training on ROI placement and data acquisition using an independent data set by a senior neuroradiologist. Axial images were analyzed on the brain window (width/center: 70/35 HU). For each VMI and conventional

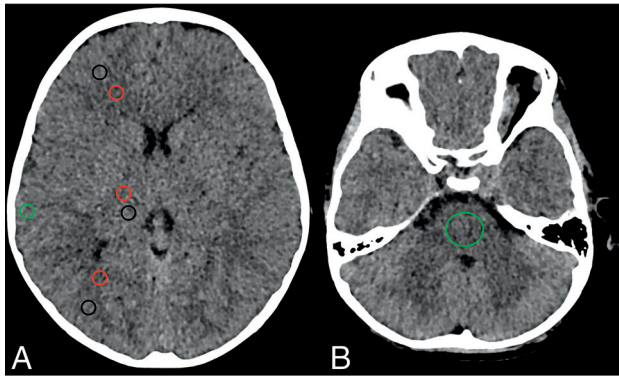


**FIG 1.** Conventional images. Placement of ROIs in cortical GM and the thalamic parenchyma (ROIs in the *black circle*), in juxtacortical WM and the posterior limb of the internal capsule (ROIs in *red circles*), as well as close to the calvaria and in the medulla oblongata (ROIs in *green circles*) on the axial plane, showing the basal ganglia (A) and the posterior fossa (B).

image data set, reader 1 placed 8 ROIs on a mid-basal ganglia section in the following anatomic locations: 1) the GM of the frontal and parietal lobes, 2) the juxtacortical WM of the frontal and parietal lobes, 3) the thalamic parenchyma, 4) the posterior limb of the internal capsule, and 5) the area near the calvaria (Fig 1A). An additional ROI was placed in the medulla oblongata (6) on the axial plane showing the petrous parts of the temporal bones, as well as the posterior fossa (Fig 1B). The locations and sizes of ROIs were identical for conventional images and VMIs. As previously described, an ROI of 25 mm<sup>2</sup> was used for all regions of the supratentorial brain versus 200 mm<sup>2</sup> for the medulla oblongata region of the posterior fossa. Patient-to-patient size-variation adjustment was performed to avoid volume averaging with the adjacent tissues. The respective CT attenuation, with an SD, was obtained from each ROI. Hounsfield unit values and image noise (SD) were averaged for comparing VMI and conventional images.

SNRs for GM and WM as well as the contrast-to-noise ratio (CNR) for GM-WM differentiation were calculated. The SNR of GM and WM for each ROI was determined as the mean CT attenuation divided by the SD. The difference was assessed as the CNR between the ROI measurements of adjacent GM and WM, as follows:  $CNR = \text{Difference of Mean CT Number between GM and WM} / \text{Square Root of the Sum of their Variances}$ .<sup>14</sup> The posterior fossa artifact index (the SD of the ROI in the posterior fossa) reflected the disturbance of attenuation values from beam-hardening and streak artifacts. The subcalvarial artifact index (SAI, the SD of the ROI close to the calvaria) served as a reference for the beam-hardening artifacts of the skull.

### Subjective Image Analysis

The subjective analysis of VMI and conventional images was performed independently by 2 radiologists, readers 2 and 3, with 3 and 5 years of experience in interpreting head CT scans, respectively, who were blinded to the applied reconstruction and scan techniques. Monoenergetic spectral images at 40, 50, 60, 70, 80, 90, and 100 keV were obtained during the reviewing process for comparing them with conventional images. The subjective

overall image quality was rated with a 5-point Likert-type scale (1 = nondiagnostic, 2 = limited, 3 = moderate, 4 = good, and 5 = excellent). Furthermore, the assessment of GM-WM matter differentiation (GWMA) was defined as the ability to distinguish GM from WM (ranging from 1 [no definite differentiation possible] to 5 [excellent differentiation]), subcalvarial space (SSA), and posterior fossa artifacts (PFAA) (ranging from 1 [no distinction of the subcalvarial space/absence of artifacts] to 5 [distinguished subcalvarial space as severe and diagnostically unacceptable]).

### Statistical Analysis

SPSS Version 19.0 (IBM), MedCalc Version 19.0.4 (MedCalc Software), and GraphPad Prism Version 7.0 (GraphPad Software) were used for data analysis. Continuous variables were expressed as mean (SD), and categorical variables, as median and range. According to the distribution pattern of continuous variables, the *t* test or Mann-Whitney *U* test was performed to compare objective evaluation indices (mean CT value, SD, SNR, CNR, posterior fossa artifact index, and SAI) between 60-keV VMIs and conventional images. The Wilcoxon test was used to compare Likert scores. Interrater agreement for subjective analysis was assessed using  $\kappa$  coefficients:  $\leq 0.20$ , poor; 0.21–0.40, fair; 0.41–0.60, moderate; 0.61–0.80, substantial; 0.81–1.00, near-perfect.  $P < .05$  was considered statistically significant.

### RESULTS

The mean patient age was 6.80 years (SD, 3.20 years), and female and male children were 42 (39.62%) and 64 (60.38%), respectively, for all age groups. The patients were 3.92 years (SD, 1.78) years and 9.38 years (SD, 1.57) years, of whom 19 (38.00%) and 23 (41.07%) were female children aged 6 years or younger and older than 6 years, respectively, and 31 (62.00%) and 33 (58.93%) were male children aged 6 years or younger and older than 6 years, respectively.

CTDI<sub>vol</sub> values were 36 and 26 mGy, and DLPs were 717.47 (SD, 41.52) mGy×cm and 520.74 (SD, 42.00) mGy×cm in the 250- and 180-mAs groups for all age groups, respectively (Table). The CTDI and DLP were significantly reduced by 28% and 28%, respectively, in the 180- and 250-mAs groups. Considering the age group (6 years or younger versus older than 6 years of age), DLP values did not differ significantly within the 250-mAs group (711.45 [SD, 47.83] mGy×cm versus 724.75 [SD, 31.8] mGy×cm;  $P = .324$ ). However, DLP values within the 180-mAs group significantly increased with age (503.76 [SD, 54.00] mGy×cm versus 531.88 [SD, 27.47] mGy×cm;  $P = .001$ ). Additionally, no significant differences in ROIs were found between the groups (ROIs for supratentorial brain in the 250- and 180-mAs groups were 25.09 [SD, 0.60] mm<sup>2</sup> and 24.90 [SD, 0.43] mm<sup>2</sup>, respectively ( $P = .064$ ). ROIs for the infratentorial brain were 199.88 (SD, 2.31) mm<sup>2</sup> and 200.4 (SD, 2.82) mm<sup>2</sup>, respectively ( $P = .30$ ).

### Objective Analysis

In the intragroup comparison of the 180- or 250-mAs groups, attenuation in the GM was significantly higher and attenuation in the WM was significantly lower in the 60-keV VMI compared with conventional images ( $P < .001$ ) for all age groups, as well as



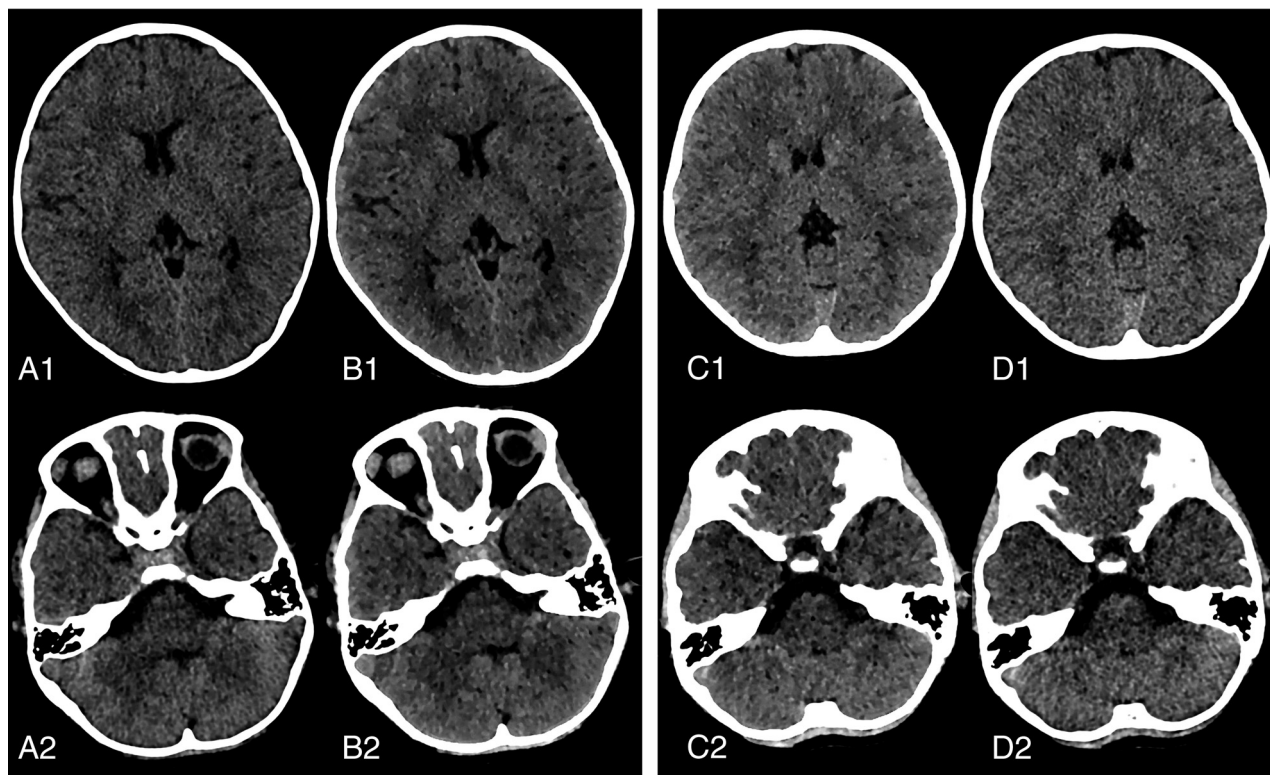


**FIG 2.** Representative images showing improved image quality in the supratentorial and infratentorial brain parenchyma for conventional images and 60-keV VMIs acquired using 250 and 180 mAs. Axial reconstruction conventional image (A) and 60-keV VMI (B) for nonenhanced brain CT scans acquired with 250 mAs in a 6-year-old girl with neuroblastoma in the retroperitoneal area. Axial reconstruction conventional image (D) and 60-keV VMI (C) for a nonenhanced brain CT scan acquired with 180 mAs in a 6-year-old girl with exotropia in the eye. GWMA (B1, C1), SSA, and PFAA (B2, C2) and overall image quality were better for 60-keV VMIs compared with conventional images (A1, D1, A2, and D2), respectively. Subjective image-quality indices were similar in 60-keV VMIs between the 250-mAs (B1, B2) and 180-mAs (C1, C2) groups. Window settings were kept identical for better comparability (level, 35; width, 70).

for the 6 years and younger and older than 6-year groups (Online Supplemental Data). Compared with conventional images, GM noise, WM noise, and PFAA were significantly lower, and GM SNR, WM SNR, and CNR were significantly higher in 60-keV VMIs ( $P < .002$ ), but SAI values were not significantly different for all age groups, as well as for the 6 years and younger or older than 6-year groups ( $P > .05$ ).

No significant differences were found in GW SNR, SAI, and CNR for 60-keV VMIs in the 250-mAs group compared with the 180-mAs group for all age groups ( $P = .064$ ,  $P = .308$ , and  $P = .150$ , respectively). GW noise, WM noise, WM SNR, SAI, and CNR were also not significantly different between the 180- and 250-mAs groups for both the 6 year and younger and older than 6-year groups ( $P > .05$ ). GM noise, WM noise, and PFAA were significantly higher and WM SNR was significantly lower in the 180-mAs group compared with the 250-mAs group for all age groups ( $P = .019$ ,  $P < .001$ ,  $P = .001$ , and  $P < .001$ , respectively). PFAA values were also significantly higher for both the 6 year and younger and older than 6-year groups ( $P = .024$  and  $P = .034$ , respectively).

### Subjective Analysis

In the intragroup comparison of both the 180- and 250-mAs groups, the assessment of GM-WM differentiation, SSA, overall

image quality, and PFAA had superior Likert scores for 60-keV VMIs compared with conventional images for all age groups, as well as for the 6 year and younger and older than 6-year groups ( $P = .013$  to  $< .001$ ; Online Supplemental Data and Fig 2). Specific to 60-keV VMIs, besides PFAA that was significantly different for the older than 6 year group ( $P = .001$ ), all indexes were not significantly different in the 250-mAs group compared with the 180-mAs group for all age groups, as well as for the 6 year and younger and older than 6-year groups (GM-WM differentiation, SSA, the overall image quality, and PFAA;  $P = .068$  to  $.686$ ,  $P = .063$  to  $.283$ ,  $P = .082$  to  $.465$ , and  $P = .055$  to  $.912$ , respectively) (Fig 2).

### Interobserver Agreement

Regarding interobserver agreement,  $\kappa$  values were 0.707 for conventional images and 0.816 for 60-keV VMIs with GWMA, 0.662 for conventional images and 0.718 for 60-keV VMIs with SSA, 0.724 for conventional images and 0.769 for 60-keV VMIs with PFAA assessment, and 0.817 for conventional images and 0.768 for 60-keV VMIs for assessing overall diagnostic quality.

### DISCUSSION

In the analysis of unenhanced brain CT images in children, by comparing image quality between 60-keV VMIs and conventional images from spectral detector CT data sets acquired with

different radiation doses, image quality for 60-keV VMIs by DLCT in the 180-mAs group was improved and the radiation dose was reduced by 28% compared with the 250-mAs group based on DLP in cranial CT.

In 60-keV VMIs, significantly higher attenuation in the GM and significantly lower attenuation in the WM were found for the same radiation dose. On the other hand, image noise was significantly lower in 60-keV VMIs compared with conventional images, irrespective of the radiation dose. This noise reduction resulted in significantly higher CNR for GM-WM differentiation on 60-keV VMIs. Hence, objective image-quality parameters were significantly better in 60-keV VMIs than in conventional images, irrespective of the DLP. Accordingly, the subjective image analysis showed a superiority for 60-keV VMIs over conventional images regarding diagnostic assessment.

Because unenhanced head CT is the imaging method of choice in patients with neurologic deficits and neurocranial traumatic lesions, there is a need for improving image quality. Previous studies found better image quality for VMIs from unenhanced head CTs due to increased GM-WM differentiation and reduced beam-hardening artifacts of the skull.<sup>22-24</sup>

A previous study using rapid-switching DECT in children reported that monoenergetic reconstruction using 60-keV resulted in better image quality because of better GM-WM differentiation and reduced artifacts in the posterior fossa.<sup>16</sup> Because this study was conducted in pediatric patients, the 60-keV VMI was selected for comparative assessment with conventional images. The outcomes supported previous studies,<sup>16,17</sup> with a superior quality obtained from 60-keV VMIs compared with conventional images. Maximal SNR and CNR and minimal noise were observed on VMIs, irrespective of radiation dose.

To the best of our knowledge, this was the first study to analyze dose reduction in children examined with 60-keV virtual monoenergetic imaging by DLCT, in which a radiation dose reduction of 28% was achieved for the CT scanning process with a tube current–time product of 180 mAs while maintaining comparable image quality versus the 250-mAs group. If one compared GW SNR, SAI, and CNR with 60-keV VMIs, the subjective analysis found no significant differences between the 250- and 180-mAs groups for all age groups; in addition, GW noise, WM noise, WM SNR, SAI, CNR, and subjective analysis were not significantly different for both the 6-year and younger and older than 6-year groups. The technique was used in adults by Reimer et al<sup>23</sup> to demonstrate a 19% reduction in radiation dose from nonenhanced head CT using DLCT by reducing the tube current without a loss of image quality. The CT scanning protocol using 180 mAs was initially selected in this study because it is considered more suitable for radiation dose reduction than CT scanning protocols using 100- and 280-mAs, respectively, as previously reported,<sup>25,26</sup> and also because approximately 20%–30% of the reduction in the radiation dose would not result in image quality not applicable for diagnosis.<sup>14</sup>

A linear relationship was demonstrated between tube current–time product and radiation dose. A decrease in tube current–time product increases image noise.<sup>27</sup> In a recent study of unenhanced head CT by Reimer et al,<sup>23</sup> image noise slightly increased from 55 to 49.8 and 44.7 mGy, respectively, showing a

significant difference between the 55- and 44.7-mGy protocols with the same reconstruction technique. Similarly, this study also revealed statistically significant increases in GW noise, WM noise, and PFAA in the 180-mAs group compared with the 250-mAs group for identical 60-keV VMIs for 0–12 years of age. However, no significant differences were observed for GW noise and WM noise in subgroup analysis based on patient age and for subjectively-rated image graininess (noise) for all age groups and age subgroups. These findings indicate that the image quality is acceptable for diagnosis, and the tube current may be further reduced without affecting image noise across age groups. Furthermore, SAI, WM SNR, and CNR were not significantly different, and there were no significant differences in overall image quality scores between the 250- and 180-mAs groups for all age groups and age subgroups.

Therefore, in this study, the degradation of image quality by such artifacts was unlikely to be significant, and overall image quality scores were similar between the 2 scan types and age subgroups. However, there was no statistically significant reduction in SAI, which indicated that our reduction of tube current to 180 mAs did not affect the objective image quality in SAI. The radiation dose for a CT scan should be carefully selected to provide optimal diagnostic image quality with the lowest possible radiation dose. Therefore, changes in the tube current–time product should be considered after consulting a radiologist, a CT technologist, and a medical physicist. In this study, radiation dose reduction was achieved by reducing the tube current–time product to 180 mAs without significantly altering the intrinsic quality of the image. Different denoising levels may impact image quality, and a medium denoising level was selected.<sup>23</sup> The effects of different denoising levels on image quality and whether the radiation dose can be reduced will be further explored.

As DLCT scanning parameters in this study, a tube voltage of 120 kV, a current of 250 mAs, a DLP of 717.47 (SD, 41.52) mGy×cm, and a CTDI<sub>vol</sub> of 36 mGy were used for conventional CT to view the pediatric brain, which were similar to or slightly lower than diagnostic reference levels for the CT radiation dose in China (804 mGy for the DLP and 39 mGy×cm for CTDI<sub>vol</sub>)<sup>28</sup> and other countries.<sup>29-34</sup> The CTDI<sub>vol</sub> is the dose of the standard American College of Radiology head phantom according to the reference phantom selection in pediatric CT;<sup>19,35</sup> the DLP is the actual radiation dose received by the patient. There was no significant difference in DLP between the 6-year and younger and older than 6-year subgroups in the 250-mAs group, while there was a significant difference in DLP between the 6-year and younger and older than 6-year subgroups in the 180-mAs group. There was a trend of DLP increase with increasing age, which may be related to head circumferences at different ages in children and head scan lengths determined by the technologist; this trend had no statistical significance between the 2 groups, with an overlap in mean DLP as observed by the SD of DLP in the 180-mAs group.<sup>36</sup> After one reduces the tube current for head CT examination, protocols can be specifically developed for various age groups because skull ossification is age-dependent.<sup>5</sup> Moreover, it was reported that CT using DLCT with spectral data does not increase the radiation dose compared with CT using DLCT without spectral data.<sup>18</sup>

There were several limitations in this study. First, this was a retrospective study performed in a single institution. The sample size was relatively small because radiation dose reduction is not performed routinely. For ethical reasons, we could not use 2 distinct CT protocols for each patient for within-subject analysis. Second, a greater reduction of the radiation dose was not evaluated though the current data suggested that this was achievable. We compared radiation doses on the basis of the DLP alone because there is no established method to normalize the radiation dose to the size of the pediatric head (unlike the size-specific dose estimates for body CT), but grouping by age was performed in this study. Third, the diagnostic value of radiation dose reduction for different brain pathologies was not evaluated because this study aimed to evaluate the possibility of radiation dose reduction while preserving overall image quality on nonenhanced brain CT comparing the 250- and 180-mAs groups. However, the evaluation of diagnostic certainty and the accuracy in pathologies is beyond the scope of this study. Finally, although the current qualitative analysis was performed in a blinded manner, an experienced reader would be likely to detect differences between conventional images and 60-keV VMIs due to differences in image texture.

## CONCLUSIONS

In this study, GM noise and WM noise, WM CNR, SAI, and CNR for supratentorial image quality were not different in objective and subjective evaluations between the 180- and 250-mAs groups, and noise in the posterior fossa differed in the objective evaluation by reduced tube current, but image quality is acceptable in the subjective evaluation, both for the 6 years and younger and the older than 6-year groups. On the basis of noise SNR, SAI, CNR, and PFAA in image analysis and observer agreement assessment, we found a dose reduction of 28% while maintaining superior image quality with a scan protocol of 180 mAs compared with 250 mAs on 60-keV VMIs from spectral detector CT in the pediatric head. These data further suggest that an even greater dose reduction is potentially achievable.

Disclosure forms provided by the authors are available with the full text and PDF of this article at [www.ajnr.org](http://www.ajnr.org).

## REFERENCES

- Hemphill JC, Greenberg SM, Anderson CS, et al; Council on Clinical Cardiology. **Guidelines for the management of spontaneous intracerebral hemorrhage: A Guideline for Healthcare Professionals From the American Heart Association/American Stroke Association.** *Stroke* 2015;46:2032–60 [CrossRef Medline](#)
- Ryan ME, Pruthi S, Desai NK, et al; Expert Panel on Pediatric Imaging. **ACR Appropriateness Criteria® Head Trauma-Child.** *J Am Coll Radiol* 2020;17:S125–37 [CrossRef Medline](#)
- Meulepas JM, Ronckers CM, Smets AM, et al. **Radiation exposure from pediatric CT scans and subsequent cancer risk in the Netherlands.** *J Natl Cancer Inst* 2019;111:256–63 [CrossRef Medline](#)
- Nelson TR. **Practical strategies to reduce pediatric CT radiation dose.** *J Am Coll Radiol* 2014;11:292–99 [CrossRef Medline](#)
- Ngo AV, Winant AJ, Lee EY, et al. **Strategies for reducing radiation dose in CT for pediatric patients: how we do it.** *Semin Roentgenol* 2018;53:124–31 [CrossRef Medline](#)
- Pearce MS, Salotti JA, Little MP, et al. **Radiation exposure from CT scans in childhood and subsequent risk of leukaemia and brain tumours: a retrospective cohort study.** *Lancet* 2012;380:499–505 [CrossRef Medline](#)
- Albert GW, Glasier CM. **Strategies for computed tomography radiation dose reduction in pediatric neuroimaging.** *Neurosurgery* 2015;77:228–32; discussion 232 [CrossRef Medline](#)
- Miglioretti DL, Johnson E, Williams A, et al. **The use of computed tomography in pediatrics and the associated radiation exposure and estimated cancer risk.** *JAMA Pediatr* 2013;167:700–07 [CrossRef Medline](#)
- McKnight CD, Watcharotone K, Ibrahim M, et al. **Adaptive statistical iterative reconstruction: reducing dose while preserving image quality in the pediatric head CT examination.** *Pediatr Radiol* 2014;44:997–1003 [CrossRef Medline](#)
- Park JE, Choi YH, Cheon JE, et al. **Image quality and radiation dose of brain computed tomography in children: effects of decreasing tube voltage from 120 kVp to 80 kVp.** *Pediatr Radiol* 2017;47:710–17 [CrossRef Medline](#)
- Nagayama Y, Nakaura T, Tsuji A, et al. **Radiation dose reduction using 100-kVp and a sinogram-affirmed iterative reconstruction algorithm in adolescent head CT: impact on grey-white matter contrast and image noise.** *Eur Radiol* 2017;27:2717–25 [CrossRef Medline](#)
- Rapp JB, Biko DM, Barrera CA, et al. **Current and future applications of thoracic dual-energy CT in children: pearls and pitfalls of technique and interpretation.** *Semin Ultrasound CT MR* 2020;41:433–41 [CrossRef Medline](#)
- Duan X, Ananthakrishnan L, Guild JB, et al. **Radiation doses and image quality of abdominal CT scans at different patient sizes using spectral detector CT scanner: a phantom and clinical study.** *Abdom Radiol (NY)* 2020;45:3361–68 [CrossRef Medline](#)
- Weinman JP, Mirsky DM, Jensen AM, et al. **Dual energy head CT to maintain image quality while reducing dose in pediatric patients.** *Clin Imaging* 2019;55:83–88 [CrossRef Medline](#)
- Ginat DT, Mayich M, Daftari-Besheli L, et al. **Clinical applications of dual-energy CT in head and neck imaging.** *Eur Arch Otorhinolaryngol* 2016;273:547–53 [CrossRef Medline](#)
- Park J, Choi YH, Cheon JE, et al. **Advanced virtual monochromatic reconstruction of dual-energy unenhanced brain computed tomography in children: comparison of image quality against standard mono-energetic images and conventional polychromatic computed tomography.** *Pediatr Radiol* 2017;47:1648–58 [CrossRef Medline](#)
- Gottumukkala RV, Kalra MK, Tabari A, et al. **Advanced CT techniques for decreasing radiation dose, reducing sedation requirements, and optimizing image quality in children.** *Radiographics* 2019;39:709–26 [CrossRef Medline](#)
- Ommen F, Jong H, Dankbaar JW, et al. **Dose of CT protocols acquired in clinical routine using a dual-layer detector CT scanner: a preliminary report.** *Eur J Radiol* 2019;112:65–71 [CrossRef Medline](#)
- Zhu X, McCullough WP, Mecca P, et al. **Dual-energy compared to single-energy CT in pediatric imaging: a phantom study for DECT clinical guidance.** *Pediatr Radiol* 2016;46:1671–79 [CrossRef Medline](#)
- Schick D, Pratap J. **Radiation dose efficiency of dual-energy CT benchmarked against single-source, kilovoltage-optimized scans.** *Br J Radiol* 2016;89:20150486 [CrossRef Medline](#)
- Ommen F, Bennink E, Vlassenbroek A, et al. **Image quality of conventional images of dual-layer SPECTRAL CT: a phantom study.** *Med Phys* 2018;45:3031–42 [CrossRef Medline](#)
- Neuhaus V, Abdullayev N, Hokamp NG, et al. **Improvement of image quality in unenhanced dual-layer CT of the head using virtual monoenergetic images compared with polyenergetic single-energy CT.** *Invest Radiol* 2017;52:470–76 [CrossRef Medline](#)
- Reimer RP, Flatten D, Lichtenstein T, et al. **Virtual monoenergetic images from spectral detector CT enable radiation dose reduction in unenhanced cranial CT.** *AJNR Am J Neuroradiol* 2019;40:1617–23 [CrossRef Medline](#)
- Lennartz S, Laukamp KR, Neuhaus V, et al. **Dual-layer detector CT of the head: Initial experience in visualization of intracranial**

- hemorrhage and hypodense brain lesions using virtual monoenergetic images. *Eur J Radiol* 2018;108:177–83 [CrossRef Medline](#)
25. Kamdem FE, Ngano SO, Alla Takam C, et al. Optimization of pediatric CT scans in a developing country. *BMC Pediatr* 2021;21:44 [CrossRef Medline](#)
  26. Tan XM, Shah MT, Chong SL, et al. Differences in radiation dose for computed tomography of the brain among pediatric patients at the emergency departments: an observational study. *BMC Emerg Med* 2021;21:106 [CrossRef Medline](#)
  27. Brenner DJ, Hall EJ. Computed tomography—an increasing source of radiation exposure. *N Engl J Med* 2007;357:2277–84 [CrossRef Medline](#)
  28. Xu H, Sun QF, Yue BR, et al. Results and analysis of examination doses for paediatric CT procedures based on a nationwide survey in China. *Eur Radiol* 2023;6:10005–7 [CrossRef Medline](#)
  29. Almén A, Guðjónsdóttir J, Heimland N, et al. Paediatric diagnostic reference levels for common radiological examinations using the European guidelines. *Br J Radiol* 2022;95:20210700 [CrossRef Medline](#)
  30. Kanal KM, Butler PF, Chatfield MB, et al. U.S. diagnostic reference levels and achievable doses for 10 pediatric CT examinations. *Radiology* 2022;302:164–74 [CrossRef Medline](#)
  31. Matsunaga Y, Chida K, Kondo Y, et al. Diagnostic reference levels and achievable doses for common computed tomography examinations: results from the Japanese nationwide dose survey. *Br J Radiol* 2019;92:20180290 [CrossRef Medline](#)
  32. Hayton A, Wallace A. Derivation of Australian diagnostic reference levels for paediatric multi detector computed tomography. *Australas Phys Eng Sci Med* 2016;39:615–26 [CrossRef Medline](#)
  33. Bondt TD, Mulkens T, Zanca F, et al. Benchmarking pediatric cranial CT protocols using a dose tracking software system: a multicenter study. *Eur Radiol* 2017;27:841–50 [CrossRef Medline](#)
  34. Ploussi A, Syrgiamiotis V, Makri T, et al. Local diagnostic reference levels in pediatric CT examinations: a survey at the largest children's hospital in Greece. *Br J Radiol* 2020;93:20190358 [CrossRef Medline](#)
  35. Chu PW, Yu S, Wang Y, et al. Reference phantom selection in pediatric computed tomography using data from a large, multicenter registry. *Pediatr Radiol* 2022;52:445–52 [CrossRef Medline](#)
  36. da Silva EH, Baffa O, Elias J jr, et al. Conversion factor for size specific dose estimation of head CT scans based on age, for individuals from 0 up to 18 years old. *Phys Med Biol* 2021;66 [CrossRef Medline](#)